

Promotion of microfracture-mediated cartilage repair by the intra-articular injection of Mg²⁺

From People's Liberation Army Joint Logistic Support Force 920th Hospital, Kunming City, China

Cite this article:
Bone Joint Res 2025;14(1):
20–32.

DOI: 10.1302/2046-3758.
141.BJR-2024-0017.R2

Correspondence should be sent to Hongbo Tan doccza@163.com

Z. Chen,^{1,2} T. Zhou,³ Z. Yin,¹ P. Duan,⁴ Y. Zhang,³ Y. Feng,¹ R. Shi,³ Y. Xu,³ R. Pang,² H. Tan³

¹Graduate School, Kunming Medical University, Kunming, China

²Basic Medical Laboratory, People's Liberation Army Joint Logistic Support Force 920th Hospital, Kunming City, Yunnan Province, China

³Department of Orthopaedics, People's Liberation Army Joint Logistic Support Force 920th Hospital, Kunming, China

⁴The First People's Hospital of Yunnan Province, Kunming, China

Aims

Magnesium ions (Mg²⁺) play an important role in promoting cartilage repair in cartilage lesions. However, no research has focused on the role of Mg²⁺ combined with microfracture (MFX) in hyaline-like cartilage repair mediated by cartilage injury. This study aimed to investigate the beneficial effects of the combination of MFX and Mg²⁺ in cartilage repair.

Methods

A total of 60 rabbits were classified into five groups (n = 12 each): sham, MFX, and three different doses of Mg²⁺ treatment groups (0.05, 0.5, and 5 mol/L). Bone cartilage defects were created in the trochlear groove cartilage of rabbits. MFX surgery was performed after osteochondral defects. Mg²⁺ was injected into knee joints immediately and two and four weeks after surgery. At six and 12 weeks after surgery, the rabbits were killed. Cartilage damage was detected by gross observation, micro-CT, and histological analysis. The expression levels of related genes were detected by real-time quantitative reverse transcription polymerase chain reaction (RT-qPCR).

Results

The histological results showed that the 0.5 mol/L Mg²⁺ group had deeper positive staining in haematoxylin-eosin (H&E), safranin O, Alcian blue, and type II collagen staining. The new cartilage coverage in the injury area was more complete, and the regeneration of hyaline cartilage was higher. The RT-qPCR results showed that sirtuin 1/bone morphogenetic protein-2/sex-determining region Y box 9 (SIRT1/BMP-2/SOX-9) and hypoxia-inducible factor 1-alpha (HIF-1α) messenger RNA levels were up-regulated after Mg²⁺ injection.

Conclusion

MFX combined with Mg²⁺ treatment has a positive effect on cartilage repair. The Mg²⁺ injection dose of 0.5 mol/L is most effective in enhancing microfracture-mediated cartilage repair.

Article focus

- Promotion of microfracture-mediated cartilage repair by the intra-articular injection of magnesium ions (Mg²⁺) in a rabbit model.

Key messages

- Intra-articular injection of Mg²⁺ after microfracture (MFX) promotes hyaline

cartilage repair and improves cartilage repair in a rabbit model.

- The Mg²⁺ injection dose of 0.5 mol/L showed a more significant improvement in cartilage repair.
- Intra-articular injection of Mg²⁺ after MFX improves cartilage repair in rabbit models, and may be related to the up-regulation of the expression of sirtuin 1/

bone morphogenetic protein-2/sex-determining region Y box 9 (SIRT1/BMP-2/SOX-9) and hypoxia-inducible factor 1-alpha (HIF-1 α).

Strengths and limitations

- This study reports for the first time that MFX combined with Mg²⁺ treatment results in a positive effect on cartilage repair.
- The staining effect of some tissue sections was poor due to the lack of correct reference method for tissue decalcification.
- In all experiments, the number of experimental animals was not continuously expanded, and large animal models used for verification were lacking due to the limitations of research funding.

Introduction

Cartilage lesions (e.g. focal cartilage defects and damage caused by cartilage degeneration) are the main cause of joint pain and disability.¹⁻⁵ The treatment of these lesions has been a challenge due to the poor self-healing capability of cartilage.⁶⁻⁹ Among cartilage lesions, microfracture (MFX) remains the most widely used clinical treatment technique.¹⁰ However, MFX easily induces the formation of fibrocartilage tissue that has poor biomechanical characteristics and tissue mechanical properties which degrade over time, resulting in poor clinical outcomes in MFX therapy patients.^{11,12} Therefore, MFX technology has been combined with cytokines, biomaterials, and chemical drug therapies to improve the repair of cartilage injury in recent years.¹² At present, some nutritional supplements, including vitamins C and D, and magnesium ions (Mg²⁺), have been reported to promote cartilage regeneration.¹³ However, the effect of combining Mg²⁺ with MFX technology on cartilage repair (especially hyaline cartilage) is unclear.

As a supplement, Mg²⁺ plays an important role in promoting cartilage repair in cartilage lesions.¹⁴⁻¹⁶ Over the past few years, Mg has been explored as a potential biomaterial for orthopaedic implants owing to its similar mechanical properties and biocompatibility to bone. Furthermore, it has been widely used in orthopaedic surgery with positive results.¹⁷ Previous studies have found that Mg²⁺ can upregulate the expression of cartilage differentiation genes and facilitate cartilage differentiation.^{18,19} In the process of chondrocyte differentiation, Mg²⁺ can promote the production of glycosaminoglycans (GAGs),²⁰ the severe deficiency of which will lead to cartilage lesions.²¹ In addition, some studies have begun to focus on the intra-articular direct injection of Mg²⁺ to improve cartilage lesions. Yao et al¹⁷ found that the injection of Mg²⁺ into joints accelerates the synthesis of cartilage matrix, inhibits inflammation, and alleviates the development of osteoarthritis. This also proves the therapeutic potential of Mg²⁺ in cartilage damage. Nevertheless, the effect of Mg²⁺ injection on MFX-mediated cartilage repair is unclear.

In this study, we evaluated the potential of intra-articular injection of Mg²⁺ after MFX in the treatment of cartilage repair. A rabbit cartilage injury model was established, and the repair effect of intra-articular injection of different concentrations of Mg²⁺ on cartilage damage after MFX treatment was detected by histological staining and gross observation.

Table 1. Primer sequences.

| Gene ID | Primer sequence |
|------------------|---------------------|
| Hif-1 α F | TTGAAGATGAAATGAAGGC |
| Hif-1 α R | ATGGTCACACGGATGGGTA |
| Sirt1 F | GAAAAACCTCCACGAACAC |
| Sirt1 R | TGGCAACTCTGACAAATGA |
| Sox9 F | CGCCCTGCCCGTC |
| Sox9 R | CCGCTCCGCCTCC |
| Bmp2 F | CCTTTGCTCGTAACCTTTG |
| Bmp2 R | CTGTTGTGTTCGCTTGA |
| Gapdh F | GGGCGGAGCCAAAAGG |
| Gapdh R | GGGTGGGCACCGGAA |

Bmp2, bone morphogenetic protein 2; F, forward; Gapdh, glyceraldehyde 3-phosphate dehydrogenase; Hif- α , hypoxia-inducible factor 1-alpha; R, reverse; Sirt1, sirtuin family member 1; Sox9, SRY-box transcription factor 9.

The possible molecular pathways after Mg²⁺ injection were explored by detecting the mRNA expression levels of several key factors in cartilage repair (sirtuin 1/bone morphogenetic protein-2/sex determining region Y box 9 (SIRT1/BMP-2/SOX-9)).

Methods

Animal model

The use of animals followed the approval of the Ethical Review Committee of the 920th Hospital of the Joint Logistics Support Force of the PLA, and complied with the institutional guidelines for the care and use of experimental animals. All animal procedures and substance administration were approved by animal protocol 2022-072-01. In this study, 60 healthy New Zealand white rabbits (aged 4 months, 2.5 to 3 kg) were randomized into five groups (n = 12 each): 1) sham group; 2) microfracture group (MFX group); 3) 0.05 mol/L group (microfracture + 0.05 mol/L injection of Mg²⁺); 4) 0.5 mol/L group (microfracture + 0.05 mol/L injection of Mg²⁺); and 5) 5 mol/L group (microfracture + 5 mol/L injection of Mg²⁺). Doses were determined based on a previous cellular study.¹³ We have included an ARRIVE checklist to show that we have conformed to the ARRIVE guidelines.

Microfracture surgery and Mg²⁺ treatment

Rabbits were injected with ceftriaxone sodium (50 mg/kg) 30 minutes before surgery to prevent infection. Then, the rabbits were anaesthetized with ketamine (40 mg/kg subcutaneously), acepromazine (0.5 mg/kg subcutaneously), and were maintained under anaesthesia by inhalation of 1% to 4% isoflurane. Next, the rabbits' fur in the surgical area was shaved and disinfected with 75% povidone iodine. A No. 15 blade was used to make a 4 to 5 cm longitudinal incision along the medial side of the patella to fully expose the femoral trochlear groove. An osteochondral defect (5 mm in diameter, 2 mm in depth) was created using a trephine on the articular cartilage of the trochlear groove.²² For the MFX

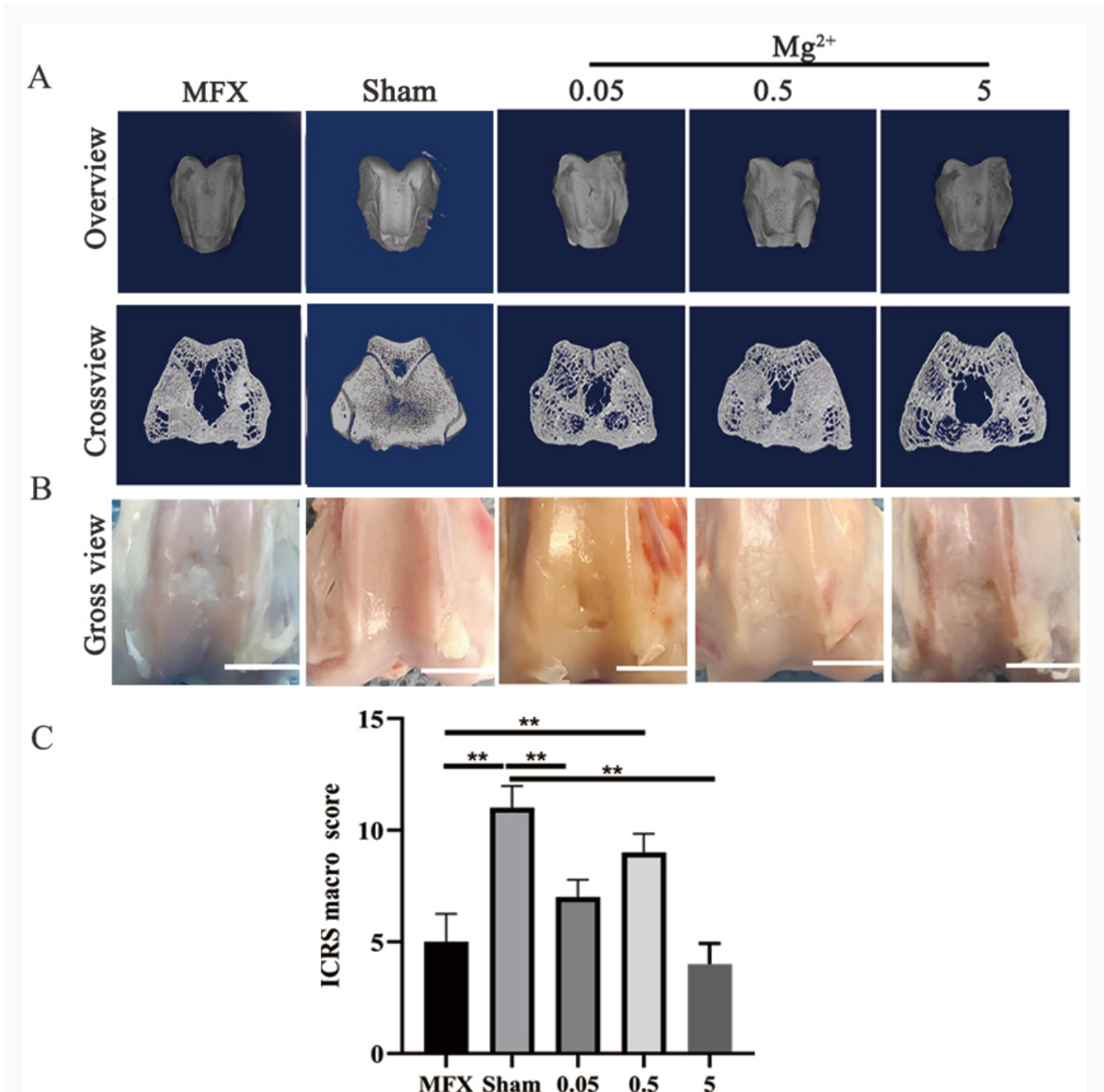


Fig. 1 Micro-CT and gross observation at six weeks after microfracture (MFX). a) Micro-CT showing the healing of subchondral bone. b) Gross image of osteochondral defect healing. c) International Cartilage Repair Society (ICRS) score. Asterisks indicate statistical significance (MFX vs Sham, $p < 0.001$; MFX vs 0.05, $p = 0.193$; MFX vs 0.5, $p = 0.003$; MFX vs 5, $p = 0.848$; Sham vs 0.05, $p = 0.003$; Sham vs 0.5, $p = 0.194$; Sham vs 5, $p < 0.001$). All p-values were calculated using independent one-way analysis of variance. * $p < 0.05$, ** $p < 0.01$). Scale bar = 5 mm; $n = 6$ rabbits per group.

group, the osteochondral defects (5 mm in diameter, 2 mm in depth) were created in the trochlear part of the rabbit knee joint with a trephine. Five holes were drilled immediately after the osteochondral defect with a 0.75 mm burr, with a hole spacing of 0.9 mm and a depth of 2 mm (care was taken not to disrupt the miniclot formed on the microfracture holes).²³ Following surgery, the wound was closed using a suture. The different concentrations of Mg^{2+} groups were injected immediately after surgery, and at two and four weeks after surgery. The sham group was injected with 1 ml physiological saline of the same volume (1 ml; M8266, Sigma Aldrich,

USA). The veterinarian of the Animal Research Office of the 920th Hospital of the Joint Logistics Support Force of the PLA provided postoperative care to the rabbits, including all animals receiving antibiotic prophylaxis (ceftriaxone sodium) for one day postoperatively. All rabbits were allowed to move freely and were housed in a stainless steel cage with a mesh bottom.

Gross observation

The New Zealand rabbits were euthanized with pentobarbital (100 to 150 mg/kg intravenously) at six and 12 weeks

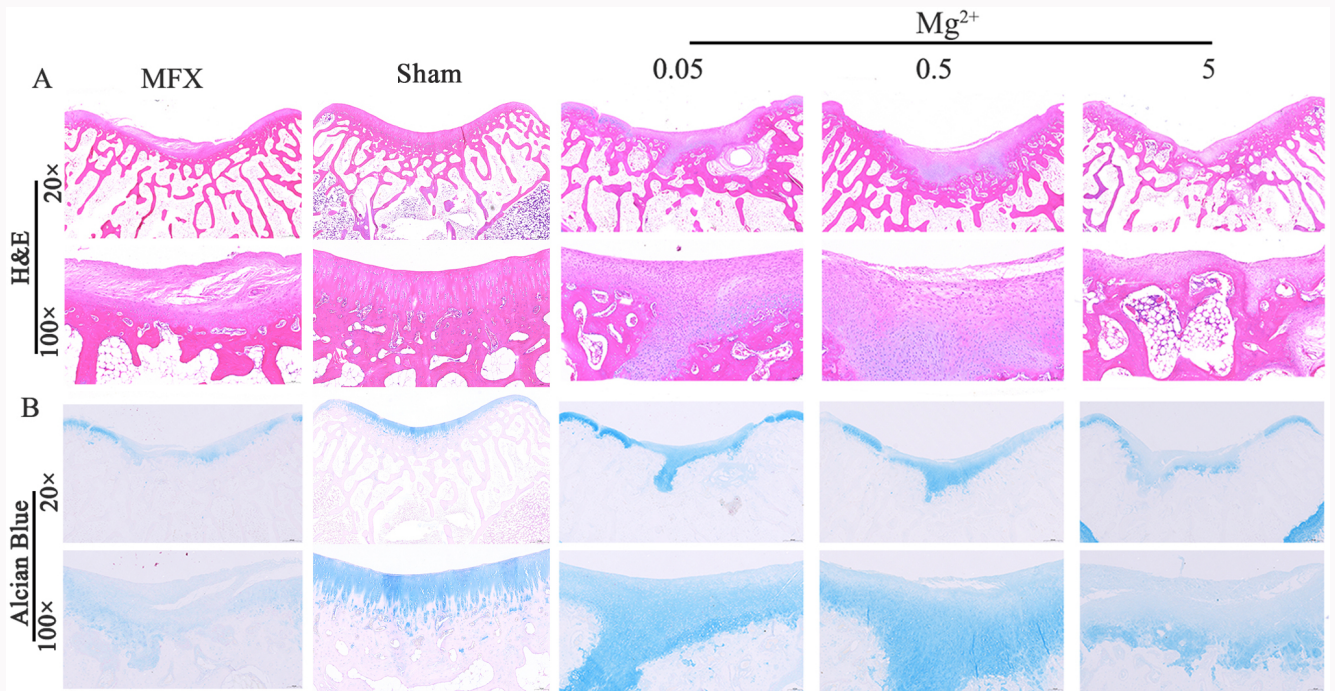


Fig. 2 Haematoxylin and eosin (H&E) staining and Alcian Blue staining at six weeks after microfracture (MFx). a) H&E staining. b) Alcian Blue staining. Scale bar = 500 μm (20 \times); scale bar = 100 μm (100 \times); n = 6 rabbits per group.

after surgery, and the distal femur was dissected immediately after euthanasia. Gross observation of the femur (macroscopic appearance was assessed using the International Cartilage Repair Society (ICRS)²⁴ macroscopic assessment scoring system) and imaged.¹⁰

Micro-CT

After micro-CT fixation, the distal femora were wrapped with paraffin film. Then, the femora were scanned using a Skyscan 1276 micro-CT instrument (Bruker micro-CT, Belgium) using the following settings: source voltage, 100 kV; source current, 200 μA ; Al + Cu filter; pixel size 20 μm ; rotation step, 0.4°. The images were then reconstructed with NRecon software (Bruker micro-CT) using the following settings: ring artifact correction, smoothing. In addition, 200 slices (4 mm) in the middle of the defect area were analyzed, and subchondral bone healing was assessed.

Histological analysis

The tissue was decalcified with 10% ethylenediaminetetraacetic acid (EDTA) plus 1% sodium hydroxide for four weeks, and after two weeks of decalcification with 5% formic acid, the dehydrated and transparent tissue block was placed in dissolved paraffin, and after the tissue block was completely immersed in paraffin, it was embedded and sliced. Sections were cut into 4 μm -thick slices and were dried and stained with haematoxylin-eosin (G1120), safranin O-fast green (G1371), and Alcian blue (G1560; all Solarbio, China). Image acquisition and analysis after panoramic scanning were conducted with an imaging system (NIKON DS-U3; Nikon, Japan).

Quantitative real-time PCR

Total RNA was extracted from fat pad tissues using TRIzol reagent (Invitrogen; Thermo Fisher Scientific, USA). Complementary DNA (cDNA) synthesis was performed using total RNA using the SureScript-First-strand-cDNA-synthesis-kit (Servicebio, China), and two doses of Universal Blue SYBR Green qPCR Master Mix Kit were used to perform qPCR on the extracted cDNA (Servicebio). Primer sequences are listed in Table I, including hypoxia-inducible factor 1- α (Hif-1 α), sirtuin family member 1 (Sirt1), SRY-box transcription factor 9 (Sox9), bone morphogenetic protein 2 (Bmp2), and glyceraldehyde 3-phosphate dehydrogenase (Gapdh). The relative levels of gene expression were expressed as ΔCt -Ct gene-Ct reference and calculated by the $2^{-\Delta\Delta\text{Ct}}$ method.

Immunohistochemistry

The tissue was decalcified with 10% EDTA plus 1% sodium hydroxide for four weeks, and after two weeks of decalcification with 5% formic acid, the dehydrated and transparent tissue block was placed in dissolved paraffin, and after the tissue block was completely immersed in paraffin, it was embedded and sliced. Sections cut into 4 μm -thick slices were dried, hydrated, permeabilized, and rinsed with 0.01 mol/L PBS (Tangier, China) solution. Antigen retrieval was conducted, the sections were blocked with 3% hydrogen peroxide, protected from light and incubated at room temperature for 25 minutes. The sections were then blocked with 10% goat serum (K5007; Dako, China), 25°C for one hour, and the appropriate concentration of primary antibody (Collagen I and Collagen II; Proteintech, USA) was added at 4°C overnight. Goat anti-rabbit universal secondary antibody (K5007; Dako) was added, corresponding to the species of the primary antibody to label the covered tissue, and incubated at room

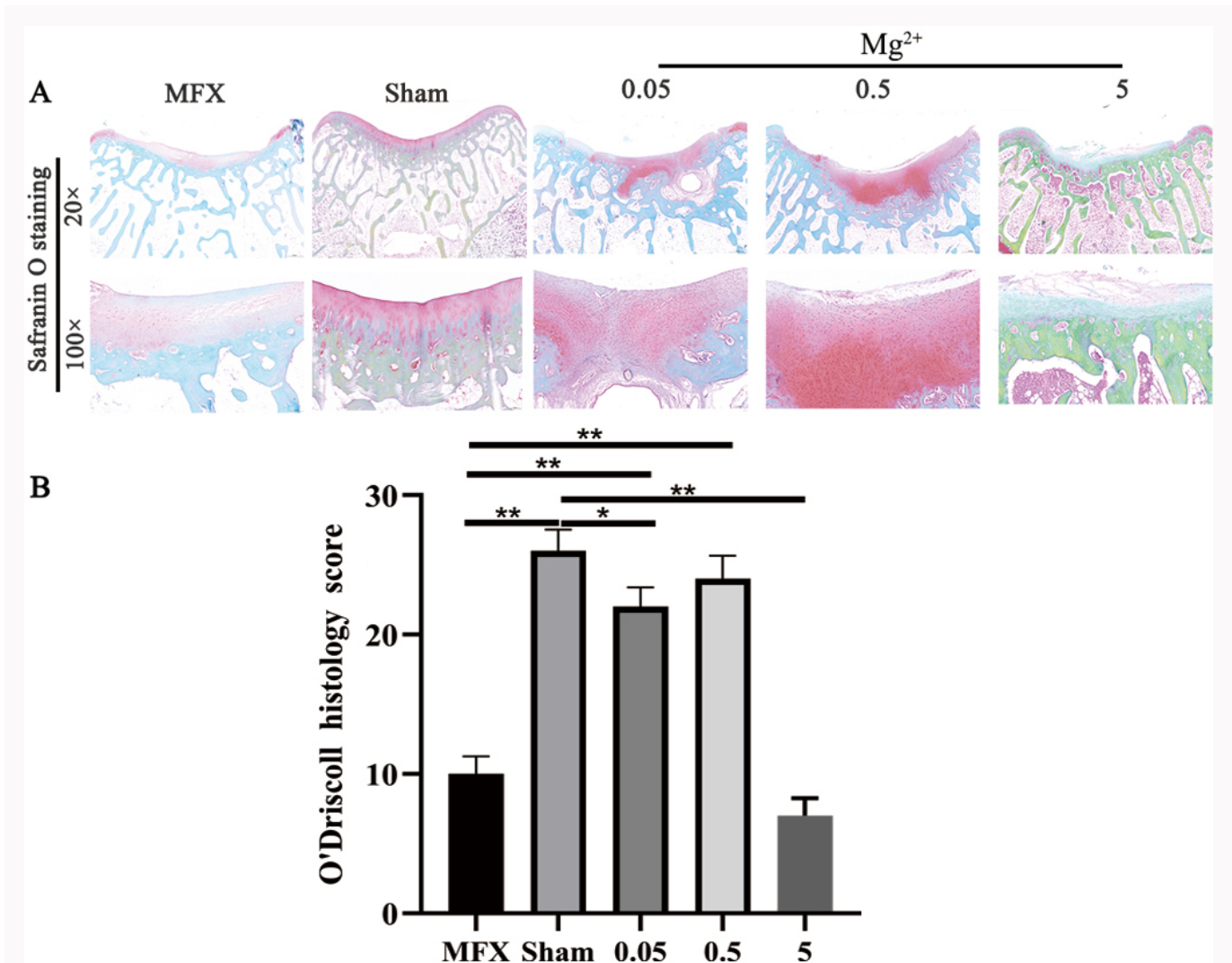


Fig. 3

Safranin O staining at six weeks after microfracture (MFX). a) Safranin O staining. b) O'Driscoll histology score. Asterisks indicate statistical significance (MFX vs Sham, $p < 0.001$; MFX vs 0.05, $p < 0.001$; MFX vs 0.5, $p < 0.001$; MFX vs 5, $p = 0.179$; Sham vs 0.05, $p = 0.044$; Sham vs 0.5, $p = 0.582$; Sham vs 5, $p < 0.001$). All p -values were calculated using independent one-way analysis of variance. * $p < 0.05$, ** $p < 0.01$). Scale bar = 500 μm (20 \times); scale bar = 100 μm (100 \times); $n = 6$ rabbits per group.

temperature for 50 minutes. Next, diaminobenzidine (DAB) colour development was conducted for five to ten minutes at room temperature, washing with distilled water. After washing with distilled water, the sections were subjected to a series of operations such as counterstaining, dehydration, transparency, and mounting. An upright fluorescence microscope (NIKON ECLIPSE E100; Nikon) was used for microscopic inspection, and an imaging system was used for panoramic scanning (NIKON DS-U3; Nikon) for image acquisition and analysis.

Statistical analysis

Statistical analysis was conducted using SPSS version 23.0 (IBM, USA). All data were presented as mean (SD). One-way analysis of variance (ANOVA) was performed for RT-qPCR. A p -value < 0.05 was considered to be statistically significant.

Results

After six weeks, the results of micro-CT showed that the MFX group and the 0.05 mol/L, 0.5 mol/L, and 5 mol/L Mg^{2+}

groups all had bone healing, but the 0.5 mol/L group showed smaller subchondral bone defects in tomograms compared to the MFX group and healed faster, while there was still a small amount of bone defects compared to the sham group (Figure 1a). Gross observation results showed that only a small amount of fibrous tissue-like structures with rough surfaces and obvious local defects were visible in the MFX group and the 5 mol/L group. In the 0.05 mol/L group, the height of the repair tissue was noticeably lower than the surrounding normal cartilage, the surface was uneven, and the boundaries of the bone defects were still clear. In the 0.5 mol/L group, a large amount of cartilage regeneration was observed. However, compared with the sham group, the quality of repair was still inferior, and the boundaries of the bone defects remained clearly visible (Figure 1b). The ICRS cartilage repair macroscopic score (Figure 1c) showed that the ICRS cartilage repair effect of the 0.5 mol/L group was significantly better than that of the MFX group ($p < 0.001$), but lower than that of the sham group.

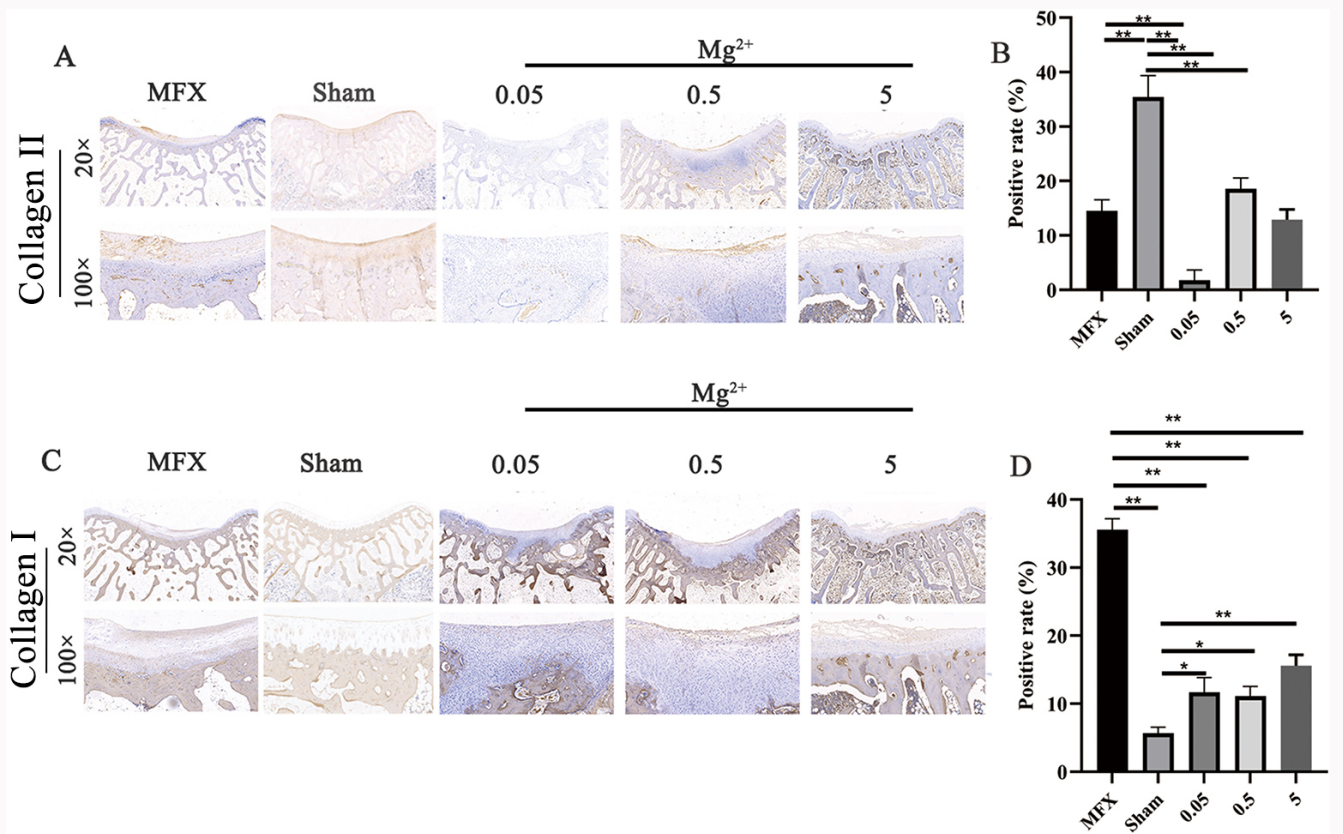


Fig. 4 a) and b) Collagen II and c) and d) collagen I staining at six weeks after microfracture (MFX), indicated by brown colour. Asterisks indicate statistical significance (collagen II: MFX vs Sham, $p < 0.001$; MFX vs 0.05, $p < 0.001$; MFX vs 0.5, $p = 0.411$; MFX vs 5, $p = 0.980$; Sham vs 0.05, $p < 0.001$; Sham vs 0.5, $p < 0.001$; Sham vs 5, $p < 0.001$; collagen I: MFX vs Sham, $p < 0.001$; MFX vs 0.05, $p < 0.001$; MFX vs 0.5, $p < 0.001$; MFX vs 5, $p < 0.001$; Sham vs 0.05, $p = 0.011$; Sham vs 0.5, $p = 0.012$; Sham vs 5, $p < 0.001$. All p -values were calculated using independent one-way analysis of variance. * $p < 0.05$, ** $p < 0.01$; Scale bar = 500 μm (20 \times). Scale bar = 100 μm (100 \times); $n = 6$ rabbits per group.

At six weeks after surgery, we performed H&E testing on the regenerated cartilage tissue. The colour of nuclei of cells was blue, and the cytoplasm was pink. At 20 \times magnification, the results showed that the MFX group, the 0.05 mol/L group, 0.5 mol/L group, and 5 mol/L group all had regenerated cartilage, and the subchondral bone was not completely healed. In the MFX group, the cartilage defects were seen on the side connected to normal cartilage. Compared with other groups, the regenerated cartilage in the 5 mol/L group was poorer. At 100 \times magnification, compared with the MFX group, 0.05 mol/L group, and 5 mol/L group, the 0.5 mol/L group healed better. In the 0.5 mol/L group, chondrocytes were evenly distributed in the cartilage layer, and the regenerated cartilage layer was visibly thicker, but compared with the sham group, the surface of regenerated cartilage in the 0.5 mol/L group was not tightly connected. In the MFX group, the surface showed intermittent filamentous continuous cartilage. In the 0.05 mol/L group, the defect repair tissue showed a natural cartilage state, and chondrocytes filled the model in the microfracture hole area, forming endochondral ossification. In the 5 mol/L group, the pink staining was not as obvious as in the other groups (Figure 2a).

Alcian blue staining was further performed on glycosaminoglycans (GAGs) after six weeks. MFX and 5 mol/L groups showed the weak positive staining of Alcian blue staining. Additionally, the 0.05 and 0.5 mol/L groups showed

more intense blue staining. Moreover, Alcian blue staining showed a fibre-like structure in the cartilage layer of the 0.05 mol/L group at higher magnification. Compared with the Sham group, the staining results showed that the cartilage layer had a minor degree of a fibre-like structure in the 0.5 mol/L group (Figure 2b).

We performed safranin O staining for GAGs, an important structural component of the cartilage matrix. At 20 \times magnification, the cartilage in the MFX group contained some proteoglycans, indicated by weak safranin O staining (weak orange-red staining). By contrast, the repaired cartilage in the 0.05 mol/L and 0.5 mol/L groups contained more proteoglycans and showed strong safranin O staining (strong orange-red staining), and the subchondral bone had not yet fully healed. In the 5 mol/L group, a small amount of regenerated cartilage was observed as weak safranin O staining (weak orange-red staining). At a higher magnification (100 \times), the MFX group showed weak safranin O staining, and the regenerated cartilage showed obvious fibrosis. In the 0.05 mol/L group, a small amount of fibrosis was observed on the surface cartilage; in the 0.5 mol/L group, a small amount of loose connective tissue was observed in the regenerated cartilage; in the 5 mol/L group, a filamentous connective tissue was observed in the regenerated cartilage (Figure 3a). O'Driscoll histology score was performed on all samples.²⁵ Compared with the MFX group, the O'Driscoll scores of the

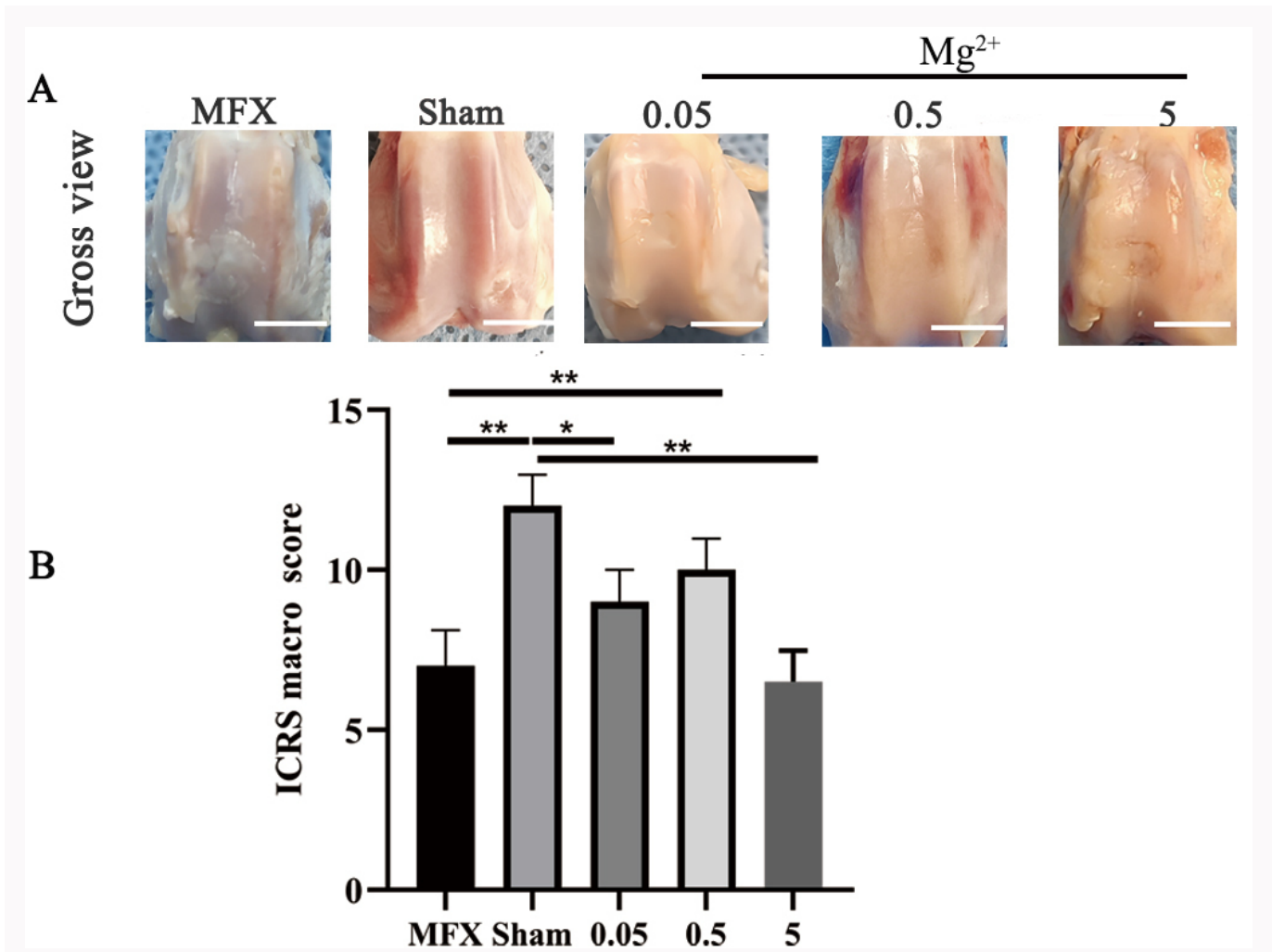


Fig. 5

Gross observation at 12 weeks after microfracture (MFX). a) Photographs of osteochondral defect healing and b) International Cartilage Repair Society (ICRS) scores. (MFX vs Sham, $p < 0.001$; MFX vs 0.05, $p = 0.087$; MFX vs 0.5, $p = 0.004$; MFX vs 5, $p = 0.999$; Sham vs 0.05, $p = 0.032$; Sham vs 0.5, $p = 0.523$; Sham vs 5, $p < 0.001$). All p -values were calculated using independent one-way analysis of variance. * $p < 0.05$, ** $p < 0.01$). Scale bar = 5 mm; $n = 6$ rabbits per group.

0.05 mol/L group and the 0.5 mol/L group were significantly upregulated. However, there was no statistical significance between the 0.5 mol/L group and the Sham group (Figure 3b).

Over 90% of the collagen in hyaline cartilage extracellular matrix (ECM) is collagen II. Our staining results for collagen II showed that this was mainly located on the cartilage surface. At 20 \times magnification, the surface of the regenerated cartilage in the MFX group showed a small amount of brown collagen II staining, and the regenerated cartilage in the cartilage defect area was not completely filled. Compared with the 0.05 mol/L group and the 5 mol/L group, the 0.5 mol/L group had more collagen II positive cartilage; but compared with the sham group, the subchondral bone in the 0.5 mol/L group was strongly stained and not completely healed. At higher magnification (100 \times), in the 0.5 mol/L group and the MFX group, the collagen II staining in the cartilage area was visible. In the MFX group, the surface of the regenerated cartilage was separated, and there were substantial gaps between the regenerated tissues, resulting in a vacuolar tissue morphology. In the 0.05 mol/L group, the regenerated cartilage was negatively stained by collagen II; in the 5 mol/L group, the cartilage surface was negatively stained by collagen II, and the

cartilage surfaces of both groups were not tightly connected (Figure 4b).

At 20 \times magnification, there was a large amount of collagen I staining on the surface of the regenerated cartilage in the MFX group; by comparison, the collagen I staining in the sham group and different Mg^{2+} concentrations was weaker. The subchondral bone in the 0.05 mol/L group and the 0.5 mol/L group was strongly stained and not completely healed. At 100 \times magnification, fibrosis occurred on the surface of the regenerated cartilage and in the centre of the subchondral bone in the MFX group. A small amount of fibrosis was seen on the surface cartilage in the 0.05 mol/L, 0.5 mol/L, and 5 mol/L groups. Quantitation results showed that there was statistical significance between the 0.5 mol/L group and the MFX and sham groups (Figure 4d).

Gross observation after 12 weeks showed that the cartilage in the defect area in the MFX, 0.05 mol/L, and 0.5 mol/L groups had nearly healed: the regenerated cartilage was the same colour as the surrounding normal cartilage. The colour difference between the regenerated cartilage in the defect area and the surrounding host cartilage in the MFX group was noticeable; a small amount of cartilage formed in

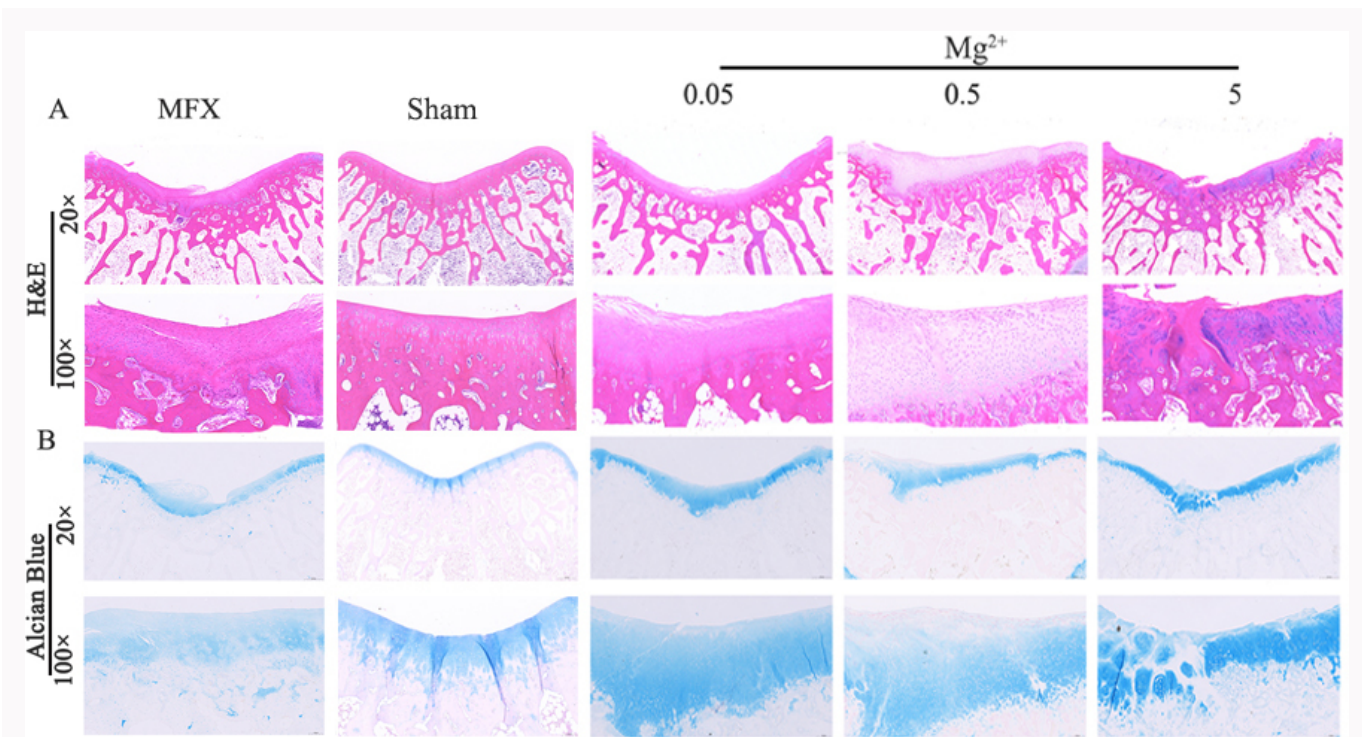


Fig. 6

Haematoxylin and eosin (H&E) staining and Alcian Blue staining at 12 weeks after microfracture (MFX). a) H&E staining; b) Alcian Blue staining; scale bar = 500 μm (20 \times). Scale bar = 100 μm (100 \times); n = 6. Each staining photograph represents the results of one rabbit from each group.

the defect area in the 5 mol/L group (Figure 5a). The ICRS score showed that there was statistical significance between the 0.5 mol/L group and the MFX group, but no statistical significance between the sham group and the 0.5 mol/L group (Figure 5b).

We performed histological H&E detection on the femora at 12 weeks. At 20 \times magnification, in the 0.5 mol/L group, the regenerated cartilage was thicker, and the interface between the new cartilage and the host cartilage was more fully integrated, but the side of the subchondral bone was not completely healed. In the MFX group, incomplete subchondral bone healing was observed. In the 0.05 mol/L group, there were substantial gaps between the regenerated tissues, resulting in a vacuolar tissue morphology. In the 5 mol/L group, the central cells of the regenerated cartilage were missing, and the subchondral bone healing was incomplete. At higher magnification (100 \times), H&E staining demonstrated that the central connection of the subchondral bone in the MFX group was discontinuous, and a small amount of adipocytes had infiltrated. In the 0.05 mol/L group, the pink bone matrix of the subchondral bone regenerated well, but the surface of the regenerated cartilage was cell-free and there was a small amount of filamentous tissue in the middle. In the 0.5 mol/L group, the regeneration was closely connected with the normal cartilage layer, compared with the sham group, and the regenerated cartilage showed most of the normal natural cartilage. In the 5 mol/L group, the connection of the cartilage layer was poor, the cell nuclei were stained darker, and the difference with the surrounding normal cartilage was greater (Figure 6a). Alcian Blue Staining illustrated that the cartilage defect area showed a thick cartilage layer at lower magnification (20 \times). In the MFX group, regenerated cartilage

punctuated connections. In the 0.05 mol/L group and the 0.5 mol/L group, subchondral bone union was incomplete. In the 5 mol/L group, positive cells were missing in the centre of the regenerated cartilage. At 100 \times magnification, the cartilage layer in the MFX group was discontinuous. There was obvious fibrosis at the cartilage surface, a few fat cells were present at the cartilage layer, and the area of defect demonstrated a cartilage that was lighter blue in colour. In the 0.05 mol/L group, dark blue cartilage was observed from the cartilage layer to the subchondral bone, a small amount of fat cells appeared in the cartilage layer, and a small amount of fibrosis appeared on the cartilage surface. In the 0.5 mol/L group, the morphology of cartilage was normal, dark blue cartilage staining was observed from the centre of the cartilage layer to the subchondral bone, and lighter blue cartilage was observed in the cartilage defect area on one side. In the 5 mol/L group, a large amount of fibrosis in the central part of the cartilage defect, dark blue cartilage, and a large number of fat cells were observed in the cartilage layer. Compared with the MFX group, the 0.5 mol/L group had the best regenerated cartilage, with a natural transparent surface and more positive cells. Compared with the sham group, the subchondral bone in the 0.5 mol/L group continued to grow dark blue (Figure 6b).

At 20 \times magnification, the middle part of the regenerated cartilage to the subchondral bone in the MFX group was positively stained, and the surface of the cartilage was colourless. Compared with the 0.05 mol/L and 5 mol/L groups, the repaired cartilage in the 0.5 mol/L group showed strong orange-red staining. In the 5 mol/L group, the orange-red staining in the centre of the regenerated cartilage was absent. At 100 \times magnification, the surface of cartilage in the MFX group showed extensive fibrosis. In the 0.05 mol/L group, the

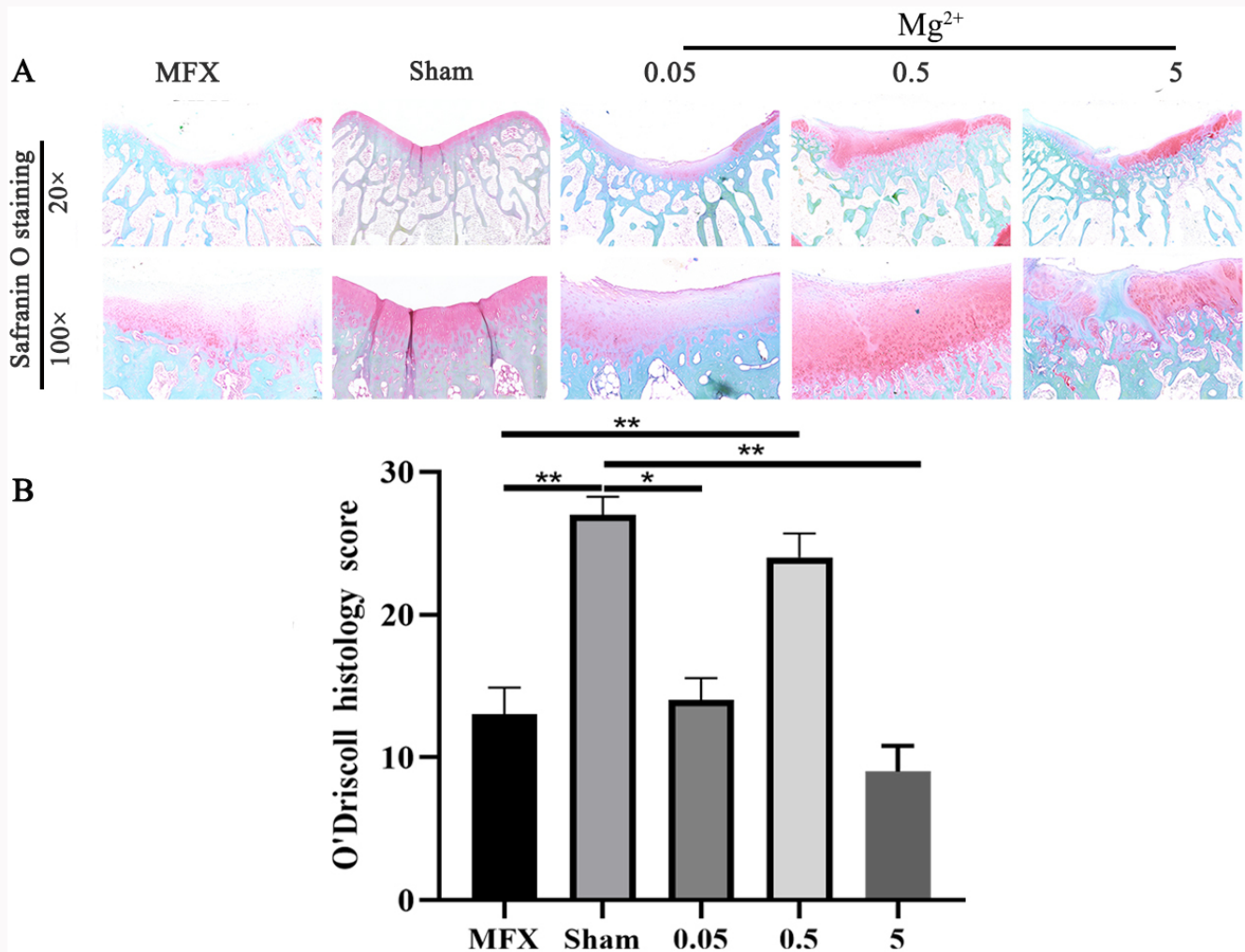


Fig. 7

Safranin O staining at 12 weeks after microfracture (MFX). a) Safranin O staining. b) O'Driscoll histology score. Asterisks indicate statistical significance (MFX vs Sham, $p < 0.001$; MFX vs 0.05, $p = 0.989$; MFX vs 0.5, $p < 0.001$; MFX vs 5, $p = 0.097$; Sham vs 0.05, $p < 0.001$; Sham vs 0.5, $p = 0.309$; Sham vs 5, $p < 0.001$. All p-values were calculated using independent one-way analysis of variance. * $p < 0.05$, ** $p < 0.01$). Scale bar = 500 μm (20 \times); scale bar = 100 μm (100 \times); $n = 6$ rabbits per group. Each Safranin O staining photograph represents the results of one rabbit from each group.

regenerated cartilage was stained orange-red, the subchondral bone had healed, and the surface of the cartilage had a small amount of reactive fibrous tissue. In the 0.5 mol/L group, the regenerated cartilage was smooth on the cartilage surface, showing an organized transparent structure. In the 5 mol/L group, fibrosis appeared in the regenerated cartilage, loss of orange-red staining was seen in the centre of the cartilage, and the cartilage connection was not tight (Figure 7a). The O'Driscoll score showed that there was statistical significance between the 0.5 mol/L group and the MFX group, but there was no statistical significance between the Sham group and the 0.5 mol/L group (Figure 7b).

After 12 weeks, the surface of the regenerated cartilage in the MFX group showed a small amount of brown collagen II staining, and the regenerated cartilage in the cartilage defect area was not completely filled; the 0.5 mol/L group had more collagen II positive cartilage than the 0.05 mol/L and 5 mol/L groups. The subchondral bone stained strongly in the 0.5 mol/L group, but had not completely healed. At higher magnification (100 \times), cracks appeared on the surface of the regenerated cartilage in the MFX group. In the

0.05 mol/L group, collagen II staining was negative. In the 0.5 mol/L group, a large amount of collagen II positive staining appeared on the cartilage surface, and a small amount of cracks appeared on the cartilage surface. In the 5 mol/L group, the staining of collagen II on the cartilage surface was negative, and a large number of cracks appeared on the cartilage surface. Quantitation results showed statistical significance between the 0.5 mol/L group and the MFX group and sham group (Figure 8b). At 20 \times magnification, a large amount of collagen II staining was observed on the surface of the regenerated cartilage in the MFX group, and compared with the MFX group the collagen II staining for different Mg^{2+} concentrations was weaker. The subchondral bone in the 0.05 mol/L group and the 0.5 mol/L group was strongly stained and not completely healed. At 100 \times magnification, fibrosis occurred on the surface of the regenerated cartilage and in the centre of the subchondral bone in the MFX group. A small amount of fibrosis was seen on the surface of cartilage in the 0.05 mol/L, 0.5 mol/L, and 5 mol/L groups. Quantitation results showed statistical significance between the 0.5 mol/L

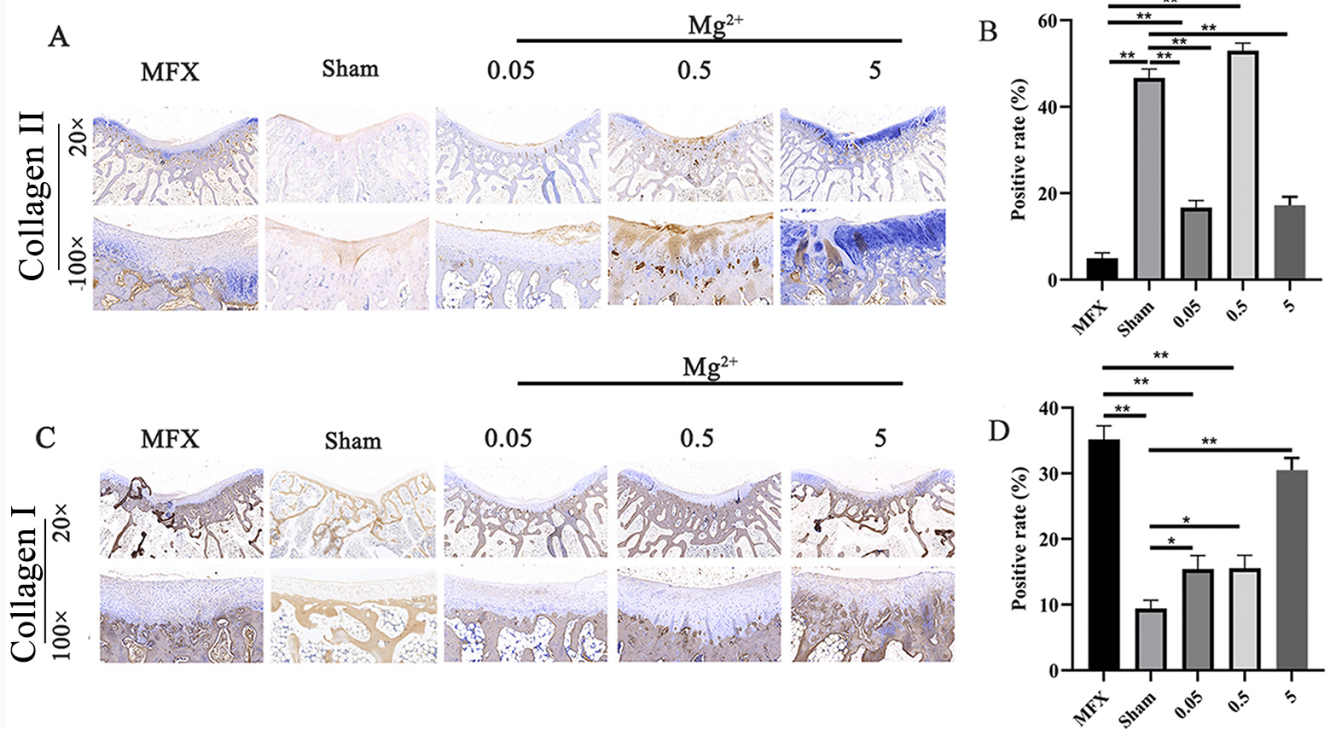


Fig. 8 Immunohistochemistry of a) and b) collagen II and c) and d) collagen I 12 weeks after microfracture (MFX). The brown colour indicates the presence of collagen I and collagen II. Asterisks indicate statistical significance (collagen II: MFX vs Sham, $p < 0.001$; MFX vs 0.05, $p < 0.001$; MFX vs 0.5, $p < 0.001$; MFX vs 5, $p < 0.001$; Sham vs 0.05, $p < 0.001$; Sham vs 0.5, $p = 0.009$; Sham vs 5, $p < 0.001$; collagen I: MFX vs Sham, $p < 0.001$; MFX vs 0.05, $p < 0.001$; MFX vs 0.5, $p < 0.001$; MFX vs 5, $p = 0.080$; Sham vs 0.05, $p = 0.019$; Sham vs 0.5, $p = 0.017$; Sham vs 5, $p < 0.001$). All p -values were calculated using independent one-way analysis of variance. * $p < 0.05$, ** $p < 0.01$). Scale bar = 500 μm (20 \times); scale bar = 100 μm (100 \times); $n = 6$ rabbits per group. Each staining photograph represents the results of one rabbit from each group.

group and the MFX group, but no statistical significance between the 0.5 mol/L group and the sham group (Figure 8d).

Effects of Mg^{2+} injection on SIRT1/BMP-2/SOX-9 and HIF-1 α

We detected the expression of SIRT1/BMP-2/SOX-9 and HIF-1 α in fat pad tissues by RT-qPCR, and the results showed that compared with the MFX group, Mg^{2+} injections significantly upregulated the expression of SIRT1, BMP-2, and SOX-9. In addition, Mg^{2+} injections significantly upregulated the expression of HIF-1 α (Supplementary Figure a).

Discussion

In this study, our results demonstrated that the intra-articular injection of Mg^{2+} after MFX can improve cartilage repair in rabbit models, which is related to the promotion of hyaline cartilage repair by Mg^{2+} . Additionally, 0.5 mol/L Mg^{2+} showed a more significant improvement in cartilage repair by histological staining and gross observation after the injection of Mg^{2+} at three concentrations (0.05, 0.5, and 5 mol/L) (Supplementary Figure b).

MFX has become the main treatment method for cartilage lesions because it features minimal trauma, low technical requirements, high surgical safety, and quick postoperative recovery. However, its long-term effect is unsatisfactory because it produces more fibrocartilage with an insufficient bearing capacity.^{26–28} Thus, combining MFX technology with cytokines, biomaterials, and chemotherapeutic drugs further stimulates the generation of hyaline cartilage

with a stronger load-bearing capacity to improve the repair ability of MFX after cartilage injury.^{29–31} While searching for a combination of MFX and drug therapies, some investigators found that the oral drug losartan combined with MFX can promote the formation of hyaline cartilage in a certain degree of cartilage damage.²² Other researchers also combined platelet-rich plasma (PRP) with MFX to promote cartilage repair.²⁹ In addition, small molecular compounds or metabolic factors play a role in MFX therapy: the injection of the small molecule compound kartogenin after MFX can improve fibrocartilage strength.³² The growth factor recombinant human fibroblast growth factor 18 (rhGF-18) partially increases hyaline cartilage formation after MFX.³³ Despite some studies on the combination therapy of MFX and drugs, the following limitations still exist. First, the concentration of drug combinations is unclear. Second, MFX has different therapeutic effects due to changes in the age of the treatment subjects. Third, small molecule compounds and metabolic growth factors have little effect in treatment. Currently, the combination of MFX and drug therapies to promote cartilage repair is still less studied, which leads to little progress. Therefore, it is important to further explore the combination of MFX and drugs to promote the research progress of cartilage repair. Drugs or supplements that can be combined with MFX treatment should be in line with current clinical standards. For this reason, Mg^{2+} has caught the attention of researchers.

In the human body, approximately half of Mg is distributed in skeletal muscle.^{34–36} The deficiency of Mg^{2+}

is associated with osteoarthritis,³⁷ osteoporosis, and other cartilage lesions.³⁸ Mg²⁺ can facilitate the repair of cartilage damage and plays an important role in human skeletal muscle. Based on this, Mg²⁺ is currently used as a supplement in conjunction with biomaterials, including hydrogels, osteochondral scaffold, etc., to repair cartilage damage.^{39,40} However, results of MFX combined with Mg²⁺ in cartilage repair have not yet been reported. Since Mg²⁺ meets the requirements of drugs or supplements combined with MFX treatment, it was hypothesized that MFX combined with Mg²⁺ treatment can also promote cartilage repair. Different concentrations of Mg²⁺ were injected intra-articularly after MFX. It was found that 0.5 mol/L Mg²⁺ can effectively increase the formation of hyaline cartilage after MFX and promote cartilage repair. After six and 12 weeks, gross observations confirmed that the regenerated cartilage in the 0.5 mol/L group recovered better, and the ICRS score of the 0.5 mol/L group was higher than that of the other experimental groups. In addition, the results of H&E staining, Alcian blue staining, and Safranin O staining all showed that the regenerated cartilage layer in the 0.5 mol/L group was visibly thicker, closely connected to the normal cartilage layer, and more GAGs were secreted. At the same time, the collagen II-positive rate in the 0.5 mol/L group was significantly higher than that in the other experimental groups. These findings may benefit the further clinical application of MFX combined with Mg²⁺ treatment.

Mg²⁺ can promote cartilage repair via several mechanisms. One previous study found that Mg²⁺ significantly upregulates the chondrogenic related gene SOX-9.¹⁹ Meanwhile, high-purity (HP) Mg has good cytocompatibility, which also promotes the expression of bone morphogenetic protein-2 (BMP-2).⁴¹ BMP-2, a key factor in the induction of chondrogenic differentiation, can induce the chondrogenic differentiation of stem cells.⁴² From the perspective of cartilage formation, the upregulation of BMP-2 and SOX-9 in chondrosis is an important signal to the promotion of cartilage formation and the alleviation of local cartilage diseases.⁴³ Furthermore, SIRT1 enhances the expression of the BMP2-induced chondrogenic differentiation factor SOX-9.⁴⁴ In this study, the mRNA expression levels of SIRT1-BMP-2/SOX-9 were detected. It was found that Mg²⁺ injection significantly upregulated the expression of SIRT1, BMP-2, and SOX-9 compared with the MFX group. Previous studies have demonstrated that HIF-1 α further induces hyaline cartilage by promoting collagen II synthesis and aggrecan formation.^{13,17,45,46} Therefore, we also examined the expression of HIF-1 α mRNA. We found that Mg²⁺ injection significantly upregulated the level of HIF-1 α mRNA. In general, MFX combined with Mg²⁺ treatment could significantly upregulate the mRNA levels of chondrogenesis-related genes SIRT1, BMP-2, and SOX-9, and increase the HIF-1 α mRNA level to promote the formation of hyaline chondrocytes.

Compared with previous studies that combined treatment with small molecule drugs or growth factors and MFX, the results of this study indicated that 0.5 mol/L Mg²⁺ combined with MFX has a better effect. The combined treatment of 0.5 mol/L Mg²⁺ and MFX was superior to that of bevacizumab and MFX in histological staining, immunohistochemical (IHC) analysis, and scoring after six weeks.¹⁰ The gross observation results were similar to those obtained by the intra-articular injection of 1 and 10 mg losartan after MFX.²²

The combined treatment of 0.5 mol/L Mg²⁺ and MFX was superior to that of PRP and MFX in gross observation, the ICRS score and histological staining results after 12 weeks.²⁹ In summary, the findings of this study establish that 0.5 mol/L Mg²⁺ combined with MFX has a positive effect on cartilage repair.

In the current study, it was demonstrated that MFX combined with Mg²⁺ treatment has a positive effect on cartilage repair. MFX combined with Mg²⁺ treatment promoted the expression of collagen II and the regeneration of hyaline cartilage. In addition, the therapeutic effect of Mg²⁺ may be linked with the upregulation of the expression of SIRT1/BMP-2/SOX-9 and HIF-1 α . The research progress of this study will inspire clinicians to explore the effective treatment measures of MFX combined with Mg²⁺ treatment to promote cartilage repair.

To conclude, MFX combined with Mg²⁺ treatment has a positive effect on cartilage repair. The Mg²⁺ injection dose of 0.5 mol/L is most effective in enhancing MFX-mediated cartilage repair.

Supplementary material

ARRIVE checklist, and bar charts showing the expression levels of related genes.

References

1. **Uzeliene I, Bironaite D, Bagdonas E, et al.** The effects of mechanical load on chondrogenic responses of bone marrow mesenchymal stem cells and chondrocytes encapsulated in chondroitin sulfate-based hydrogel. *Int J Mol Sci.* 2023;24(3):2915.
2. **Khurana A, Nejadnik H, Gawande R, et al.** Intravenous ferumoxylol allows noninvasive MR imaging monitoring of macrophage migration into stem cell transplants. *Radiology.* 2012;264(3):803–811.
3. **Karami P, Stampoultzis T, Guo Y, Pioletti DP.** A guide to preclinical evaluation of hydrogel-based devices for treatment of cartilage lesions. *Acta Biomater.* 2023;158:12–31.
4. **Helwa-Shalom O, Saba F, Spitzer E.** Regeneration of injured articular cartilage using the recombinant human amelogenin protein. *Bone Joint Res.* 2023;12(10):615–623.
5. **Jun Z, Yuping W, Yanran H, et al.** Human acellular amniotic membrane scaffolds encapsulating juvenile cartilage fragments accelerate the repair of rabbit osteochondral defects. *Bone Joint Res.* 2022;11(6):349–361.
6. **Fortier LM, Knapik DM, Dasari SP, et al.** Clinical and magnetic resonance imaging outcomes after microfracture treatment with and without augmentation for focal chondral lesions in the knee: a systematic review and meta-analysis. *Am J Sports Med.* 2023;51(8):2193–2206.
7. **Sennett ML, Friedman JM, Ashley BS, et al.** Long term outcomes of biomaterial-mediated repair of focal cartilage defects in a large animal model. *Eur Cell Mater.* 2021;41:40–51.
8. **Migliorini F, Maffulli N, Baroncini A, Bell A, Hildebrand F, Schenker H.** Autologous matrix-induced chondrogenesis is effective for focal chondral defects of the knee. *Sci Rep.* 2022;12(1):9328.
9. **Shim DW, Hong H, Lee JW, Kim BS.** Particulated autologous cartilage transplantation for the treatment of osteochondral lesion of the talus: can the lesion cartilage be recycled? *Bone Jt Open.* 2023;4(12):942–947.
10. **Utsunomiya H, Gao X, Cheng H, et al.** Intra-articular injection of bevacizumab enhances bone marrow stimulation-mediated cartilage repair in a rabbit osteochondral defect model. *Am J Sports Med.* 2021; 49(7):1871–1882.
11. **Solheim E, Hegna J, Inderhaug E, Øyen J, Harlem T, Strand T.** Results at 10–14 years after microfracture treatment of articular cartilage defects in the knee. *Knee Surg Sports Traumatol Arthrosc.* 2016;24(5):1587–1593.

12. Mustapich T, Schwartz J, Palacios P, Liang H, Sgaglione N, Grande DA. A novel strategy to enhance microfracture treatment with stromal cell-derived factor-1 in a rat model. *Front Cell Dev Biol.* 2020;8:595932.
13. Yao H, Xu J, Wang J, et al. Combination of magnesium ions and vitamin C alleviates synovitis and osteophyte formation in osteoarthritis of mice. *Bioact Mater.* 2021;6(5):1341–1352.
14. Lozo E, Riecke K, Schwabe R, Vormann J, Stahlmann R. Synergistic effect of ofloxacin and magnesium deficiency on joint cartilage in immature rats. *Antimicrob Agents Chemother.* 2002;46(6):1755–1759.
15. Li Z, Zheng X, Wang Y, et al. The biomimetics of Mg²⁺-concentration-resolved microenvironment for bone and cartilage repairing materials design. *Biomimetics (Basel).* 2022;7(4):227.
16. Zhao J, Wu H, Wang L, et al. The beneficial potential of magnesium-based scaffolds to promote chondrogenesis through controlled Mg²⁺ release in eliminating the destructive effect of activated macrophages on chondrocytes. *Biomater Adv.* 2022;134:112719.
17. Yao H, Xu JK, Zheng NY, et al. Intra-articular injection of magnesium chloride attenuates osteoarthritis progression in rats. *Osteoarthritis Cartilage.* 2019;27(12):1811–1821.
18. Hu T, Xu H, Wang C, Qin H, An Z. Magnesium enhances the chondrogenic differentiation of mesenchymal stem cells by inhibiting activated macrophage-induced inflammation. *Sci Rep.* 2018;8(1):3406.
19. Yue J, Jin S, Gu S, Sun R, Liang Q. High concentration magnesium inhibits extracellular matrix calcification and protects articular cartilage via Erk/autophagy pathway. *J Cell Physiol.* 2019;234(12):23190–23201.
20. Hagandora CK, Tudaes MA, Almarza AJ. The effect of magnesium ion concentration on the fibrocartilage regeneration potential of goat costal chondrocytes. *Ann Biomed Eng.* 2012;40(3):688–696.
21. Gruber HE, Ingram J, Norton HJ, et al. Alterations in growth plate and articular cartilage morphology are associated with reduced SOX9 localization in the magnesium-deficient rat. *Biotech Histochem.* 2004;79(1):45–52.
22. Logan CA, Gao X, Utsunomiya H, et al. The beneficial effect of an intra-articular injection of losartan on microfracture-mediated cartilage repair is dose dependent. *Am J Sports Med.* 2021;49(9):2509–2521.
23. Kraeutler MJ, Aliberti GM, Scillia AJ, McCarty EC, Mulcahey MK. Microfracture versus drilling of articular cartilage defects: a systematic review of the basic science evidence. *Orthop J Sports Med.* 2020;8(8):2325967120945313.
24. Mainil-Varlet P, Aigner T, Brittberg M, et al. Histological assessment of cartilage repair: a report by the Histology Endpoint Committee of the International Cartilage Repair Society (ICRS). *J Bone Joint Surg Am.* 2003;85-A Suppl 2:45–57.
25. Koshino T, Wada S, Ara Y, Saito T. Regeneration of degenerated articular cartilage after high tibial valgus osteotomy for medial compartment osteoarthritis of the knee. *Knee.* 2003;10(3):229–236.
26. Becher C, Malahias MA, Ali MM, Maffulli N, Thermann H. Arthroscopic microfracture vs. arthroscopic autologous matrix-induced chondrogenesis for the treatment of articular cartilage defects of the talus. *Knee Surg Sports Traumatol Arthrosc.* 2019;27(9):2731–2736.
27. Guo T, Noshin M, Baker HB, et al. 3D printed biofunctionalized scaffolds for microfracture repair of cartilage defects. *Biomaterials.* 2018;185:219–231.
28. Escalante S, Rico G, Becerra J, et al. Chemically crosslinked hyaluronic acid-chitosan hydrogel for application on cartilage regeneration. *Front Bioeng Biotechnol.* 2022;10:1058355.
29. Yang Z, Wu Y, Yin K, et al. The therapeutic value of arthroscopic microfracture technique in combination with platelet-rich plasma injection for knee cartilage injury. *Am J Transl Res.* 2021;13(4):2694–2701.
30. Truong M-D, Choi BH, Kim YJ, Kim MS, Min B-H. Granulocyte macrophage – colony stimulating factor (GM-CSF) significantly enhances articular cartilage repair potential by microfracture. *Osteoarthritis Cartilage.* 2017;25(8):1345–1352.
31. Browe DC, Burdis R, Díaz-Payno PJ, et al. Promoting endogenous articular cartilage regeneration using extracellular matrix scaffolds. *Mater Today Bio.* 2022;16:100343.
32. Xu X, Shi D, Shen Y, et al. Full-thickness cartilage defects are repaired via a microfracture technique and intraarticular injection of the small-molecule compound kartogenin. *Arthritis Res Ther.* 2015;17(1):20.
33. Power J, Hernandez P, Guehring H, Getgood A, Henson F. Intra-articular injection of rhFGF-18 improves the healing in microfracture treated chondral defects in an ovine model. *J Orthop Res.* 2014;32(5):669–676.
34. Wang K, Wei H, Zhang W, et al. Severely low serum magnesium is associated with increased risks of positive anti-thyroglobulin antibody and hypothyroidism: a cross-sectional study. *Sci Rep.* 2018;8(1):9904.
35. Hosseini Dastgerdi A, Ghanbari Rad M, Soltani N. The therapeutic effects of magnesium in insulin secretion and insulin resistance. *Adv Biomed Res.* 2022;11:54.
36. Franke VL, Breitling J, Ladd ME, Bachert P, Korzowski A. ³¹P MRSI at 7 T enables high-resolution volumetric mapping of the intracellular magnesium ion content in human lower leg muscles. *Magn Reson Med.* 2022;88(2):511–523.
37. Veronese N, Stubbs B, Maggi S, et al. Dietary magnesium and incident frailty in older people at risk for knee osteoarthritis: an eight-year longitudinal study. *Nutrients.* 2017;9(11):1253.
38. Castiglioni S, Cazzaniga A, Albisetti W, Maier JAM. Magnesium and osteoporosis: current state of knowledge and future research directions. *Nutrients.* 2013;5(8):3022–3033.
39. Luo M, Chen M, Bai J. A bionic composite hydrogel with dual regulatory functions for the osteochondral repair. *Colloids Surf B Biointerfaces.* 2022;219:112821.
40. Bonifacio MA, Cometa S, Cochis A, et al. A bioprintable gellan gum/lignin hydrogel: a smart and sustainable route for cartilage regeneration. *Int J Biol Macromol.* 2022;216:336–346.
41. Cheng P, Han P, Zhao C, et al. High-purity magnesium interference screws promote fibrocartilaginous entheses regeneration in the anterior cruciate ligament reconstruction rabbit model via accumulation of BMP-2 and VEGF. *Biomaterials.* 2016;81:14–26.
42. Murphy MP, Koepke LS, Lopez MT, et al. Articular cartilage regeneration by activated skeletal stem cells. *Nat Med.* 2020;26(10):1583–1592.
43. Cha B-H, Kim J-H, Kang S-W, et al. Cartilage tissue formation from dedifferentiated chondrocytes by codelivery of BMP-2 and SOX-9 genes encoding bicistronic vector. *Cell Transplant.* 2013;22(9):1519–1528.
44. Lu Y, Zhou L, Wang L, et al. The role of SIRT1 in BMP2-induced chondrogenic differentiation and cartilage maintenance under oxidative stress. *Aging (Albany NY).* 2020;12(10):9000–9013.
45. Stegen S, Laperre K, Eelen G, et al. HIF-1 α metabolically controls collagen synthesis and modification in chondrocytes. *Nat New Biol.* 2019;565(7740):511–515.
46. Vinatier C, Merceron C, Guicheux J. Osteoarthritis: from pathogenic mechanisms and recent clinical developments to novel prospective therapeutic options. *Drug Discov Today.* 2016;21(12):1932–1937.

Author information

Z. Chen, MD, Orthopaedic Surgeon, Graduate School, Kunming Medical University, Kunming, China; Basic Medical Laboratory, People's Liberation Army Joint Logistic Support Force 920th Hospital, Kunming City, Yunnan Province, China.

T. Zhou, MD, Professor in Orthopaedic Surgery
Y. Zhang, MSc, Orthopaedic Surgeon
R. Shi, MD, Orthopaedic Surgeon
Y. Xu, MD, Professor in Orthopaedic Surgery

H. Tan, MD, Associate Head of Orthopaedic Surgery
Department of Orthopaedics, People's Liberation Army Joint Logistic Support Force 920th Hospital, Kunming, China.

Z. Yin, MSc, Orthopaedic Surgeon
Y. Feng, MSc, Orthopaedic Surgeon
Graduate School, Kunming Medical University, Kunming, China.

P. Duan, Medical Student, Research Fellow, The First People's Hospital of Yunnan Province, Kunming, China.

R. Pang, MD, Professor of Immunology, Basic Medical Laboratory, People's Liberation Army Joint Logistic Support Force 920th Hospital, Kunming City, Yunnan Province, China.

Author contributions

Z. Chen: Formal analysis, Investigation, Writing – original draft, Writing – review & editing.
T. Zhou: Formal analysis, Investigation, Writing – review & editing.
Z. Yin: Formal analysis, Writing – review & editing.
P. Duan: Formal analysis, Writing – review & editing.
Y. Zhang: Formal analysis, Writing – review & editing.
Y. Feng: Investigation, Writing – review & editing.
R. Shi: Investigation, Writing – review & editing.
Y. Xu: Investigation, Writing – review & editing.
R. Pang: Conceptualization, Writing – review & editing.
H. Tan: Conceptualization, Writing – original draft, Writing – review & editing.

R. Pang and H. Tan contributed equally to this work.

Funding statement

The authors disclose receipt of the following financial or material support for the research, authorship, and/or publication of this article: this work was supported by the National Natural Science Foundation of China (31970515).

ICMJE COI statement

This study was supported by the National Natural Science Foundation of China (31970515).

Data sharing

The data that support the findings for this study are available to other researchers from the corresponding author upon reasonable request.

Ethical review statement

The use of animals followed the approval of the Ethical Review Committee of the 920th Hospital of the Joint Logistics Support Force of the PLA (2022-072-01).

Open access funding

The open access fee for this article was provided by the National Natural Science Foundation of China (31970515).

© 2025 Chen et al. This is an open-access article distributed under the terms of the Creative Commons Attribution Non-Commercial No Derivatives (CC BY-NC-ND 4.0) licence, which permits the copying and redistribution of the work only, and provided the original author and source are credited. See <https://creativecommons.org/licenses/by-nc-nd/4.0/>